A Comparison of Phase Organization of Model Segmented Polyurethanes with Different Intersegment Compatibilities

Rebeca Hernandez,[‡,†] Jadwiga Weksler,[§] Ajay Padsalgikar,[§] Taeyi Choi,[†] Elena Angelo,[†] J. S. Lin,[||] Li-Chong Xu,[⊥] Christopher A. Siedlecki,[⊥] and James Runt*[,†]

Center for the Study of Polymeric Systems, Department of Materials Science and Engineering, The Pennsylvania State University, University Park, Pennsylvania 16802, AorTech Biomaterials, Dalmore Drive, Caribbean Park, Scoresby, VIC 3179 Australia, Oak Ridge National Laboratory, Oak Ridge, Tennessee 37831, and Departments of Surgery and Bioengineering, Milton S. Hershey Medical Center, Hershey, Pennsylvania 17033

Received June 29, 2008; Revised Manuscript Received October 9, 2008

ABSTRACT: Three series of chemically well-defined polyurethanes were synthesized with the same hard segments but different soft-segment chemistries of interest in biomedical applications. The multiblock polyurethanes have soft segments composed of either an aliphatic polycarbonate [poly(1,6-hexyl 1,2-ethyl carbonate)], polytetramethylenoxide, or a mixed macrodiol of polyhexamethylenoxide and hydroxyl-terminated poly(dimethylsiloxane) and the same hard-segment chemistry [4,4′-methylenediphenyl diisocyanate and 1,4-butanediol]. Analysis using small-angle X-ray scattering and other methods demonstrates that demixing of the hard and soft segments varies greatly between the three series of copolymers. For example, the PDMS/PHMO-based copolymers exhibit a three-phase, core−shell morphology, while the other two series exhibit a typical two-phase structure. In addition to quantitative measurements of hard/soft-segment demixing for the two-phase copolymers, FTIR spectroscopy was used to assess inter- and intracomponent hydrogen bonding, and tapping mode AFM was used to characterize the nanoscale morphology.

1. Introduction

Three principle factors are well-known to influence the formation of the phase-separated microstructure of segmented polyurethane (PU) block copolymers: block lengths, their chemical composition, and associated thermodynamic miscibility between hard and soft segments.[1,2] For a fixed composition, block length, and overall molecular weight, Velankar and Cooper[3] demonstrated that changing miscibility between hard and soft segments results in materials ranging from nearly homogeneous to strongly microphase separated. Hard segments composed of methylene bis(*p*-phenyl isocyanate) (MDI) and 1,4-butanediol (BDO), the focus of the current investigation, can interact with chemically complimentary soft segments, leading to higher degrees of unlike segment mixing. For example, early studies demonstrated that poly(ester urethanes) exhibit a higher degree of hard/soft-segment mixing compared with poly(ether urethanes), due to relatively strong hydrogen bonding between the urethane N−H groups and polyester carbonyls.[4,5]

Another example of the importance of intersegment hydrogen bonding in multiblock PUs are those containing aliphatic polycarbonate soft segments, in which polycarbonate carbonyls can form relatively extensive hydrogen bonding with urethane N−H groups.[6] Tang et al.[7] have reported microphase separation using small-angle X-ray scattering (SAXS) experiments for a polyurethane containing aliphatic polycarbonate soft segments (PCU, hard-segment content = 30 wt %); the mean interdomain spacing was determined to be 22 nm. Revenko et al.[8] confirmed the presence of microphase separation in similar PCU copolymers using tapping mode atomic force microscopy (AFM), although the phase morphology was rather ill-defined. The PCU investigated in their study clearly exhibited a two-phase morphology consisting of hard-segment-rich and soft-segment-rich phases. Upon magnification of what the authors refer to as the "soft-segment phase", rodlike hard domains (about 50 nm in length) were visible throughout the soft domain matrix. Christenson et al. also observed a similar morphology in the commercial PCU Corethane 80A [equivalent to Bionate 80A]; its hard-segment content has been reported elsewhere to be around 35 wt %.[9] The hard domains in the latter investigation were observed to be cylindrical, ∼5−10 nm in width and 40−100 nm in length, a scale comparable to that reported by Revenko et al.[8] and a number of other AFM studies of segmented PUs and poly(urethane urea)s having different soft-segment chemistries.[10,11] In contrast, other authors have reported that hard and soft segments in similar PCUs are essentially mixed, as demonstrated by the results of DSC experiments.[6] Hard/soft-segment miscibility was attributed to hydrogen-bond formation between the carbonyl groups of the soft segments and urethane amide groups in hard segments.

Use of highly apolar macrodiols (such as polybutadiene, polyisobutylene, and polydimethylsiloxane) as soft segments in PUs leads to highly phase separated solid-state structures, arising from the immiscibility of the hard and soft segments (i.e., the absence of reasonably strong intersegment interactions).[12−17] One way of increasing segmental "compatibility" between highly apolar macrodiols and MDI−BDO (and similar hard segments) is by chemical modification of one or both blocks. For example, controlled epoxidation of diene soft segments after synthesis has been shown to increase soft-segment polarity, enhancing miscibility with PU hard segments.[18] Another example is the introduction of polar cyanoethyl side groups along an apolar siloxane backbone to promote miscibility with hard segments.[19] The introduction of a second macrodiol, such as PTMO[12] or polyhexamethylenoxide PHMO,[20] with intermediate polarity between siloxane units and PU hard segments is another method to increase intersegment "compatibility".

* To whom correspondence should be addressed. E-mail: runt@matse.psu.edu.
† The Pennsylvania State University.
‡ Present address: Instituto de Ciencia y Tecnologia de Polimeros, CSIC, Madrid, Spain.
§ AorTech Biomaterials.
|| Oak Ridge National Laboratory.
⊥ Milton S. Hershey Medical Center.

10.1021/ma8014454 CCC: $40.75
Published on Web 11/19/2008

In a recent paper, we proposed a model to describe the structural organization of segmented polyurethanes synthesized from MDI−BDO and a mixed macrodiol (PDMS/PHMO) in which the PDMS constitutes 80 wt % of the soft segment. These polymers organize into three phases: hard domains, siloxane domains, and a mixed phase composed of the second macrodiol, PDMS end-group segments, and dissolved hard-segment sequences.[21] Due to the presence of three phases, quantification of the degrees of phase separation by the Bonart and Muller[22,23] approach, extensively applied for treating small-angle X-ray scattering of polyurethanes[24] and polyurethaneureas,[25,26] is not appropriate in this case.

In this paper, we seek to compare the structural organization of three series of well-defined polyurethanes having the same hard-segment chemistry, but with different soft-segment chemistries of particular interest in biomedical applications: aliphatic polycarbonate, polytetramethylenoxide, and mixed PDMS/PHMO macrodiols. The phase-separation characteristics of the hard segments and the polyether mixed phase in the case of PUs synthesized from a mixed macrodiol (PDMS/PHMO) are explored through Fourier transform infrared (FTIR) spectroscopy and the findings compared with the hydrogen bonding observed for poly(carbonate urethanes) and poly(tetramethylenoxide urethanes), for which the degree of phase separation can be quantitatively obtained from SAXS experiments by using the approach of Bonart and Mueller. Earlier studies on polyurethanes with MD−BDO hard segments and a copolymer of PPO−PEO (MW = 2000) as the soft segments reported a degree of phase separation obtained from SAXS experiments that ranged from 0.2 for copolymers with a 30 wt % hard-segment concentration to 0.37 for samples with 60 wt % hard-segment concentration (with 0 indicating no phase separation and 1 indicating complete phase separation between hard and soft segments). At hard-segment concentrations higher than 60 wt %, the degree of phase separation decreased with hard-segment content, presumably due to kinetic constraints in packing the hard-segment sequences.[24] A more recent study[27] on segmented polyurethanes with the same chemical composition of the hard segments (MDI−BDO) and (3000 MW) PPO−PEO soft segments found that the overall degree of phase separation was almost constant (around 0.65) for hard-segment concentrations ranging from 50 to 90 wt %. To our knowledge, quantification of the degree of phase separation of PHEC and PTMO soft segment MDI−BDO polyurethanes has not been reported previously.

2. Experimental Section

2.1. Reagents. The starting materials were methylene bis(*p*-phenyl isocyanate) (MDI) and 1,4-butanediol (BDO) for the hard segments, and these were purchased from Sigma Aldrich (98% purity). Three different soft-segment chemistries were considered (see Figure 1):[28] poly(tetramethyleneoxide) diol (M_w = 1000, obtained from Urethane Compounds) and poly(1,6-hexyl 1,2-ethyl carbonate) diol (PHEC, M_w = 1000, obtained from UBE Industries), and a mixed macrodiol composed of hydroxyterminated poly(dimethylsiloxane) (M_w = 1000) and poly(hexamethylenoxide) diol (M_w = 700) (both synthesized by AorTech Biomaterials), in a ratio of 80/20 w/w. The polydispersity index of all macrodiols was found to be approximately 1.5 and the purities were all >97%. The hydroxy-terminated poly(dimethylsiloxane) was subjected to rigorous fractional distillation on a thin film evaporator. The distilled material was then evaluated using gas chromatography to ensure that all low molecular weight cyclics were removed.

2.2. Synthesis and Hard Segment Length Distribution. PUs with varying hard-segment contents were synthesized via a two-step process (i.e., the so-called prepolymer method). In general, a prepolymer was prepared by carefully adding MDI to a reaction vessel containing the appropriate macrodiol, and the BDO was subsequently added for chain extension. The PTMO and PDMS/PHMO [the latter using a mixed macrodiol (PDMS/PHMO (80/20) (w/w))] copolymer series was synthesized using a bulk procedure,[20] while the PHEC copolymers were synthesized in solution in *N*,*N*-dimethylacetamide (DMAc, LC grade, 99%, Biolab Australia, minimum 99% purity). The principle reason the PHEC-based materials were solution polymerized was to follow the same two-step addition scheme. Without a solvent, we could not prepare the PHEC PUs using a two-step process. Once the solvent is removed, the materials are melt processable.

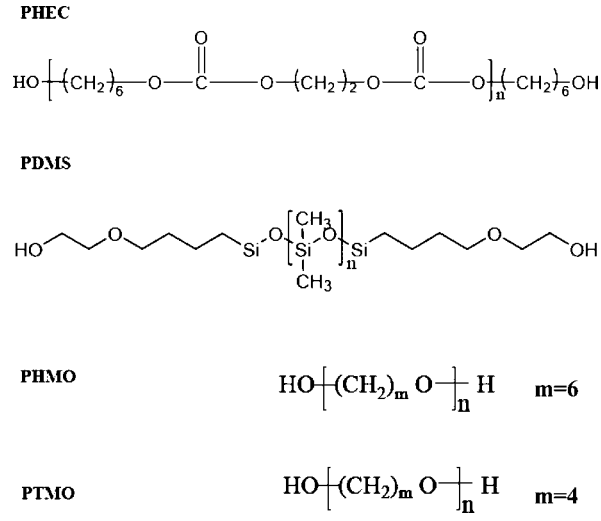

Figure 1. Chemical structures of the PU soft segments under consideration.

Three series of PUs were prepared: (PDMS/PHMO)−PUs (series I) with the following hard-segment contents, 30 wt % ((PDMS/PHMO)-30), 32.5 wt % ((PDMS/PHMO)-32.5), 35 wt % ((PDMS/PHMO)-35), 40 wt % ((PDMS/PHMO)-40), 45 wt % ((PDMS/PHMO)-45), and 52 wt % ((PDMS/PHMO)-52); PHEC−PUs (series II) with PHEC as the soft segment with the following hard-segment contents (PU designation in parentheses), 32.5 wt % (PHEC-32.5), 40 wt % (PHEC-40), 45 wt % (PHEC-45), and 52 wt % (PHEC-52); and PTMO−PUs (series III) with PTMO as the soft segment with the following hard-segment contents, 32.5 wt % (PTMO-32.5), 40 wt % (PTMO-40), 45 wt % (PTMO-45), and 52 wt % (PTMO-52). The hard-segment length distributions were computed according to Peebles,[29] and the results obtained for all the series are equivalent, since the statistical procedure does not depend on the soft-segment chemistry.

The calculated hard-segment sequence length distributions for the (PDMS/PHMO)−PU copolymers are displayed in Figure 2. The probabilities were normalized by the number of MDI residues in the *i*-mer (i + 1) and by the initial concentration of MDI used for the (PDMS/PHMO)−PU. The normalized probabilities were then multiplied by the weight of that sequence to obtain a weight average. The distribution shows that the most probable segment lengths are only a 1-mer (one BDO units and two MDI units) for copolymers with a hard-segment concentration lower than 40 wt %, a 2-mer (two BDO units and three MDI units) for copolymers with 45 wt % hard segments, and a 3-mer (three BDO units and four MDI units) for copolymers with 52 wt % hard segments. Figure 2 also illustrates that the likelihood of lone MDIs is reduced by raising the hard-segment content. Moreover, higher concentrations of hard segments introduce longer sequence lengths into the copolymers, which are favorable for promoting microphase separation.

Films of 120−140 μm thickness were cast from 20−30% solutions of the polymers in DMAc and heated at 55 °C for 16−18 h. The cast films are further dried under vacuum at 40 °C for another 24 h before evaluation.

2.3. Small-Angle X-ray Scattering (SAXS). SAXS data were collected on a Molecular Metrology SAXS instrument consisting of a three-pinhole collimated camera [using a Cu Kα radiation

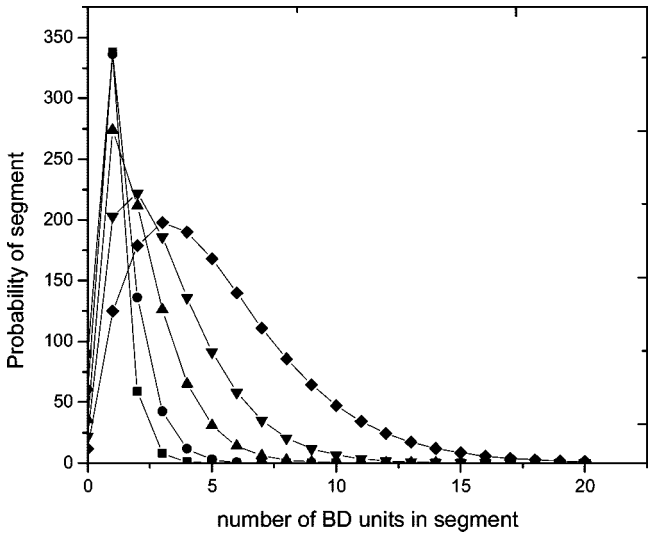

Figure 2. Normalized weight average hard-segment sequence length distribution for PU copolymers: ■, 30 wt % hard segments; ●, 35 wt %; ▲, 40 wt %; ▼, 45 wt %; ◆, 52 wt %.

source ($\lambda = 0.154$ nm)] and a two-dimensional multiwire detector. The sample-to-detector distance was 1.5 m.

The PU films were cut into 1 cm × 1 cm squares, which were stacked to a thickness of approximately 1 mm and secured by tape along the edges. The film stack was supported by placing it between two index cards with a hole for the passage of the X-ray beam. The ensemble was then mounted onto a sample holder provided by Molecular Metrology.

Absolute scattered intensities (in units of cm^{-1}) were determined by calibration with a precalibrated cross-linked polyethylene (S-2907) secondary standard; this step is essential in order to obtain quantitative details on segment demixing.[29] A silver behenate secondary standard was used to calibrate the scattering vector.

Quantification of the degree of phase separation via SAXS experiments involves comparison of a hypothetical electron density variance for the case of complete segment separation, with the experimentally determined variance. The theoretical electron density variance of a completely phase separated two-phase system is defined as

$$\overline{\Delta\eta_c^2} = \phi_{hs}\phi_{ss}(\eta_{hs} - \eta_{ss})^2 \quad (1)$$

where ϕ_{hs} and ϕ_{ss} are the volume fractions and η_{hs} and η_{ss} the electron densities of the hard and soft segments, respectively.

Experimental variances are related to the SAXS invariant (Q, the total scattered intensity) by a constant, c

$$\overline{\Delta\eta^2} = cQ = c\int_0^\infty I(q)q^2\,dq \quad (2)$$

where

$$c = \frac{1}{2\pi^2 i_e N_A^2} = 1.76\times10^{-24}\ \text{mol}^2/\text{cm}^2 \quad (3)$$

and i_e is Thompson's constant for the scattering from one electron (7.94×10^{-26} cm^2). N_A is Avogadro's number.

Experimental variances ($\overline{\Delta\eta^{2\prime}}$) are calculated simply from the background corrected SAXS intensities. They incorporate mixing in the microdomains and the influence of diffuse phase boundaries. The ratio of the experimental variance to the hypothetical completely phase separated variance ($\overline{\Delta\eta^{2\prime}}/\overline{\Delta\eta_c^2}$) provides a measure of the overall degree of phase separation. This ratio returns a value between 0 and 1, with unity indicating complete phase separation and infinitely sharp phase boundaries.

This model is applied for the case of PTMO- and PHEC-based copolymers. (PDMS/PHMO)-based copolymers exhibit three phases, and therefore this model is not appropriate in this case. Two different approaches have been adopted to model the scattering from the three-phase system. A pseudo-two-phase model can be assumed if (a) the electron density of one of the phases does not significantly contribute to the sample scattering and (b) its contribution is embedded in one of the other two phases. The pseudo-two-phase model can be applied appropriately to analyze SAXS data of the (PDMS/PHMO)−PU with a high hard-segment concentration ≥40 wt %. For these compositions, eq 1 is appropriate to obtain the experimental variance assuming that phase 1 is the siloxane phase and phase 2 is a mixed phase composed of hard segments mixed with PHMO and PDMS end-group segments.

The second approach is based on a modified hard sphere scattering model that has been extensively applied to interpretate the scattering patterns of ionomers [referred to as the Yarusso−Cooper (Y−C) model]

$$I(q) = I_e(q)V\frac{1}{V_P}F^2(q)\frac{1}{1+(8V_{ca}/V_p)\varepsilon\Phi(2qR_{ca})} \quad (4)$$

where ε is a constant ∼ 1, R_{ca} is the radius of closest dispersed phase approach, and $V_{ca} = 4/3\pi R_{ca}^3$. This model is valid for copolymers with hard-segment concentrations less than 40 wt %, in which complete phase separation between the hard domains and the polyether phase is assumed. More details are given in ref 21.

2.4. Tapping Mode AFM. The copolymer sample surfaces were imaged using a multimode AFM with Nanoscope IIIa control system (software version 5.2r3, Veeco Instruments, Santa Barbara, CA), operating in tapping mode with phase imaging detection. All images were acquired under ambient conditions over a controlled series of tapping forces ranging from r_{sp} values of 0.5 to 0.9, where $r_{sp} = A/A_o$ (set point amplitude/free amplitude of oscillation) and higher r_{sp} corresponds to lighter tapping forces that are more surface sensitive. The amplitude of free oscillation was kept constant at 20 nm for all images. Topographic and phase data were recorded simultaneously with a standard silicon tapping tip (Vista, Nanoscience Instruments, Phoenix, AZ) on a beam cantilever. Phase imaging data were extracted and analyzed through Gaussian fitting with Microcal Origin 6.0 software. These results were used to analyze the size of hard domains using Scion Image software (Scion Corp.).

2.5. Fourier Transform Infrared (FTIR) Spectroscopy. FTIR spectroscopy was performed on a Bio-Rad FT-6 spectrometer. PU solutions (∼3% w/w) in DMAc were cast onto KBr discs and then dried overnight at room temperature before drying them at 80 °C for 1 h under vacuum. Each sample was scanned 64 times at a resolution of 2 cm^{-1}. Curve fitting on the carbonyl stretching region was performed in a manner similar to that described previously for polyurethanes[30] and polyamides[31] for all of the copolymers. A truncated area of the carbonyl region was chosen as to avoid the effect of any absorptions in the wings of the band envelope. An iterative least-squares computer program was used to obtain the best fit of the experimental data by varying the frequency (ν), width at half-height (w), and intensity of the Gaussian bands (A). The areas corresponding to the hydrogen-bonded carbonyl groups were corrected by taking into account the differences in absorptivity between the free and hydrogen-bonded carbonyl groups. The absorptivity ratio, calculated by Painter et al.[30] for a model polyurethane, is $k = 1.71$ and the concentration of carbonyl groups was determined by dividing the area corresponding to each absorbance by the total area corresponding to the carbonyl region.

2.6. Thermal Analysis (DSC). Phase transitions of the copolymers were determined using a TA-Q100 DSC. Each sample was first cooled to −90 °C, heated at a rate of 10 °C/min up to 250 °C, cooled at −90 °C at a heating rate of 100 °C/min, and then reheated again at 250 °C at a heating rate of 10 °C/min.

3. Results and Discussion

3.1. Phase Morphology. Figure 3 illustrates 500 nm × 500 nm AFM phase microscopy images of the (PDMS/PHMO)-40 copolymer obtained with increasing tapping force: from r_{sp} =

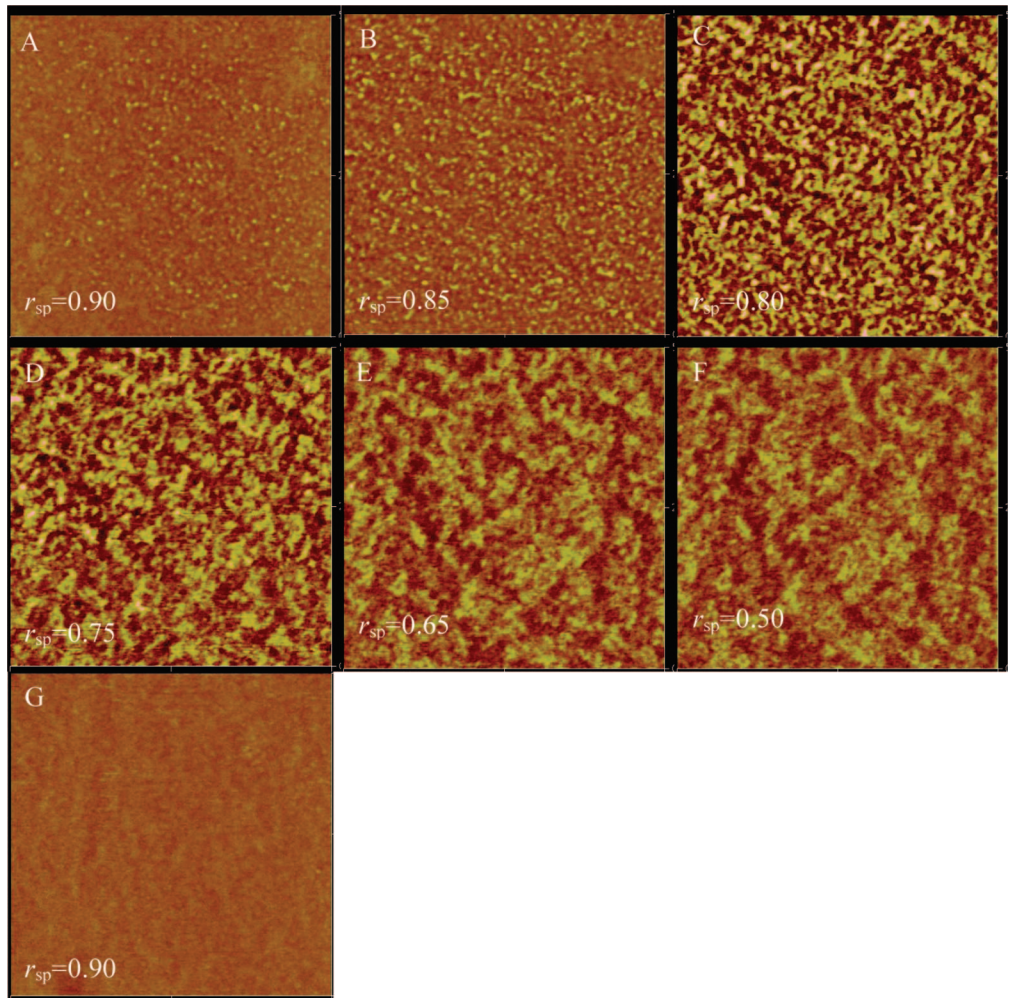

Figure 3. (A−F) AFM phase images of (PDMS/PHMO)-40 at different tapping forces r_{sp} from 0.90 to 0.50. (G) AFM phase image of PTMO-40 at light tapping force $r_{sp} = 0.90$. Scan size: 500 × 500 nm^2. Phase scale: 20°.

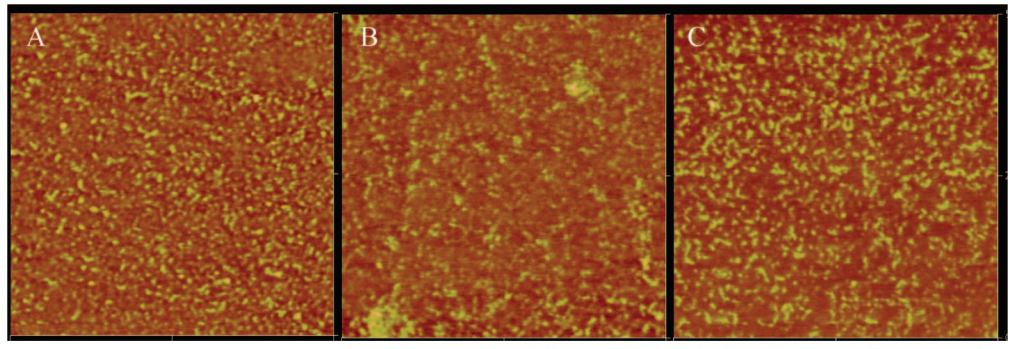

Figure 4. AFM phase images of (A) (PDMS/PHMO)-40, (B) PTMO-40, and (C) PHEC-40 at tapping force $r_{sp} = 0.85$. Scan size: 500 × 500 nm^2. Phase scale: 20°.

0.9 (Figure 3A) to 0.5 (Figure 3F). Note that increasing amounts of hard domains (denoted by the bright regions) are observed with increasing tapping force, similar to previous observations.[10] This arises from the projection of the three-dimensional volume of detection (with increasing z-depth, as r_{sp} decreases) into the two-dimensional phase image. Note that even at the lowest tapping force for which stable imaging could be obtained with the (PDMS/PHMO)-40 polymer ($r_{sp} = 0.9$), some hard domains can be observed. In contrast, PTMO-40 imaged at this same r_{sp} displays no hard domains (Figure 3G), consistent with this surface being composed of either a thicker soft-segment overlayer under ambient conditions or, alternatively, that PDMS is somewhat easier to "tap through" than the PTMO soft segment. At increasing tapping force, domains appear to increase in size as more also appear. Eventually, the image becomes enriched in hard domains so that contrast between the different regions begins to disappear and the surface begins to appear increasingly homogeneous. Very similar results were observed for the PTMO and PHEC copolymers, and these images are not shown.

Figure 4 displays phase images of the three copolymers [(PDMS/PHMO), PTMO and PHEC] with 40 wt % hard segment at $r_{sp} = 0.85$. The peak value was used as the threshold to differentiate between hard and soft domains, and the hard domains were analyzed by image analysis software. Analysis of the hard domains showed them to be predominantly cylindri-

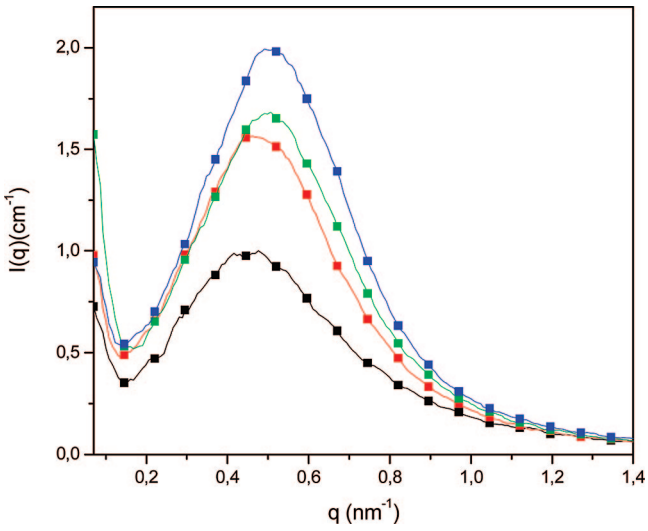

Figure 5. Background-corrected SAXS intensities as a function of scattering vector for (black squares) PHEC-32.5, (red squres) PHEC-40, (green squares) PHEC-45, and (blue squres) PHEC-52.

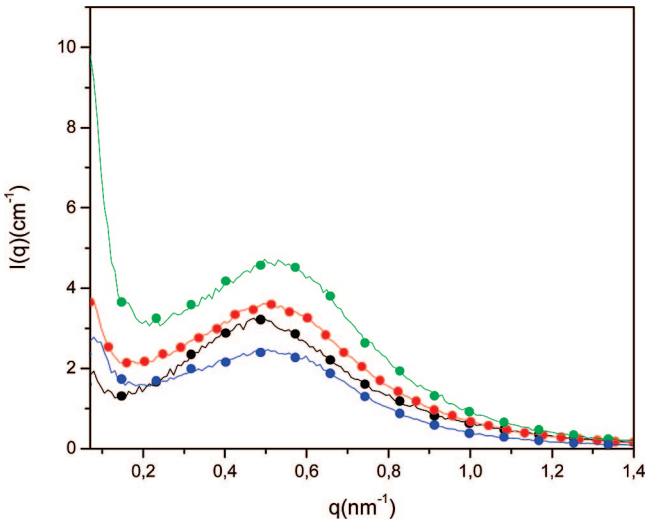

Figure 6. Background-corrected SAXS intensities as a function of the scattering vector for (black circles) PTMO-32.5, (red circles) PTMO-40, (green circles) PTMO-45, and (blue circles) PTMO-52.

cal for all three materials shown in Figure 4, with occasional spheroid-like domains observed. It is not clear if these objects are truly spheres or clusters of hard domains, as observed in ref 10. Quantitative analysis of the dimensions of the hard domains using a uniform $r_{sp} = 0.85$ resulted in an average dimension of 47 nm^2 for (PDMS/PHMO)-40. However, it should be noted that there was a large range of domains sizes observed, with maximum areas up to 400 nm^2 for this sample. Analysis of PTMO-40 showed a remarkably similar mean value of 50 nm^2 but with a maximum domain area of 1310 nm^2, while PHEC-40 had a mean domain size of 76 nm^2 and a maximum value of 3380 nm^2.

3.2. Degrees of Phase Separation. Background scattering corrected SAXS spectra for PHEC−PUs and PTMO−PUs are presented in Figures 5 and 6, respectively. The experimental SAXS data for the (PDMS/PHMO)−PUs have been reported in a previous publication.[21]

Peak positions (q_{max}), indicative of mean interdomain spacings between hard domains ($d = 2\pi/q_{max}$), are displayed in Table 1. For the PHEC−PUs, the interdomain spacings decrease slightly with the HS content from 13.5 nm (32.5 wt %) to 12.2 nm (52 wt %). This small change is in the same range as that reported in ref 32 for polyether soft segment PUs in which the interdomain spacing was reported to change from 11.7 nm (30 wt %) to 9.9 nm (50 wt %). In the case of PTMO−PUs, the interdomain spacing does not vary with composition within the limits of the experimental uncertainty.

Table 1. Interdomain Spacings, Electron Density Variances, And Degrees of Microphase Separation for the PU Copolymers under Consideration

	interdomain spacing (nm)	$\overline{\eta_c}^2 \times 10^{3a}$ (mol e$^-$/cm^3)^2	$\overline{\eta}^{2\prime} \times 10^{3b}$ (mol e$^-$/cm^3)^2	deg of microphase separation ($\overline{\eta}^{2\prime}/\overline{\eta_c}^2$)
		PHEC−PUs		
PHEC-32.5	13.5	3.62	0.40	0.11
PHEC-40	13.0	4.17	0.54	0.13
PHEC-45	12.5	4.67	0.61	0.13
PHEC-52	12.2	4.94	0.70	0.14
		PTMO−PUs		
PTMO-32.5	13.0	4.49	1.38	0.31
PTMO-40	13.0	5.19	1.53	0.29
PTMO-45	12.6	5.86	2.07	0.35
PTMO-52	13.6	6.26	0.98	0.16
		(PDMS/PHMO)−PUs		
(PDMS/PHMO)-30	8.6			
(PDMS/PHMO)-32.5	8.8			
(PDMS/PHMO)-35	10.3			
(PDMS/PHMO)-40	8.8	2.30	2.24	∼1
(PDMS/PHMO)-45	9.6	2.44	2.91	∼1
(PDMS/PHMO)-52	10.8	2.62	2.59	∼1

[a] Theoretical electron variance obtained according to eq 1. [b] Experimental electron variance obtained according to eq 2.

(PDMS/PHMO)−PUs exhibit a lower interdomain spacing than PTMO−PUs and PHEC−PUs for all hard-segment concentrations. Except for (PDMS/PHMO)-35, d increases slightly with increasing hard-segment content. The interpretation of the dependence of the peak position based on hard/soft block miscibility is not at all straightforward if the block length polydispersity is not quantitatively known,[33,34] as is the case with the three series under investigation here. Koberstein and Stein[32] proposed a model to explain the phase organization of segmented polyurethanes with polydisperse hard block lengths, in which at any temperature only blocks that are longer than a certain length microphase separate. Although, as noted later, the microphase separated structure of the (PDMS/PHMO)−PUs is more complex than the PTMO and PHEC copolymers, the smaller mean spacings observed for the (PDMS/PHMO)−PUs are consistent with a smaller "cut off" block length for microphase separation, arising from the immiscibility of MDI−BDO and the (PDMS/PHMO) portion of the soft segments.

Calculated degrees of phase separation as determined by the ratio of the experimental variance to the hypothetical completely phase separated variance ($\overline{\Delta\eta^{2\prime}}/\overline{\Delta\eta_c^2}$) are displayed in Table 1 for the three series of PU copolymers. The presence of three phases in (PDMS/PHMO)−PUs prevents the quantification of the degree of phase separation via the general Bonart and Mueller approach[22,23] that considers two phases: hard and soft domains. Nevertheless, we have shown previously[21] that a pseudo-two-phase model can be used to treat the scattering data of (PDMS/PHMO)−PUs with hard-segment concentrations ≥40 wt %. The theoretical (completely phase separated) variances for these copolymers are then calculated by considering a soft phase composed of siloxane units and a pseudohard phase composed of hard domains and PHMO and PDMS end-group segments. Degrees of phase separation were found to be close to 1 for all (PDMS/PHMO) copolymers with hard-segment concentrations ≥40 wt %, indicating the formation of a completely separated siloxane phase.[21] At hard-segment con-

centrations lower than 40 wt %, a modified core−shell model is instead employed to model the SAXS data.[21] The formation of a completely separated siloxane phase has also been verified for hard-segment concentrations lower than 40 wt % through dynamic mechanical analysis and wide-angle X-ray scattering experiments.[21]

For PTMO−PUs and PHEC−PUs, the Bonart and Mueller approach that considers a soft phase (composed of PTMO or PHEC, lone MDI units, and some dissolved, relatively short, hard segments) and a hard phase composed of hard segments is appropriate for all compositions. Details of the calculation of the theoretical variances are provided in the accompanying Supporting Information.

The results in Table 1 demonstrate that there is a significant degree of mixing of unlike segments for the PTMO and, particularly, the PHEC copolymers. The degrees of phase separation for the PHEC−PUs remain the same or perhaps increase slightly with increasing hard-segment content. The degree of phase separation for PTMO−PUs reaches a maximum for PTMO-45, similar to earlier results that demonstrated the influence of kinetic constraints on segment demixing for PU copolymers with higher hard-segment concentrations.[26] As noted earlier, the (PDMS/PHMO)−PUs exhibit a three-phase microstructure, and at ≥40 wt % hard segments we demonstrated previously that a pseudo-two-phase model is appropriate.[21] A degree of phase separation of approximately 1 (in Table 1) indicates that within experimental uncertainty all of the PDMS segments are phase separated from the other components of these copolymers.

Except for PTMO-52, in which demixing kinetics strongly influence phase separation, PTMO−PUs exhibit a significantly higher degree of phase separation than PHEC−PUs. The solubility parameters calculated by using a group contribution method[35] are 11.9 ± 0.4 (cal cm^{-3})$^{1/2}$ for hard segments composed of one BDO and two MDI units and 8.8 ± 0.4 and 9.2 ± 0.4 for PTMO and PHEC pure soft segments, respectively. Since the solubility parameter differences between hard and soft segments of the PTMO and PHEC copolymers are the same within experimental uncertainty, this difference in degrees of phase separation arises from differences in intersegment hydrogen bonding, as described in the next section.

3.3. FTIR Spectroscopy: Hydrogen Bonding. The hydrogen-bonding characteristics of segmented polyurethanes have been extensively studied in the past using FTIR spectroscopy. This technique has been used occasionally to estimate degrees of phase separation for PU copolymers, based on the idea that the quantity of hydrogen-bonded carbonyls can be related to the extent of hard-segment bonding in hard domains.[36] We do not, however, attempt to quantitatively compare our SAXS results with those from FTIR for two reasons. Films used in FTIR experiments are relatively thin in order to comply with Beer's law, and thus it is unclear if the observed behavior is representative of the bulk, as evaluated by SAXS.[10,25,37] There is also concern whether the solidification history is precisely the same as that experienced by the SAXS samples. SAXS degrees of phase separation are defined by including both diffuse boundaries and segment intermixing, while for the case of FTIR, strongly hydrogen-bonded carbonyls very likely reside only in hard domains and thus would not be influenced by diffuse boundaries.

FTIR spectra corresponding to the carbonyl region of PHEC−PUs for all hard-segment concentrations are presented in Figure 7. Aliphatic polycarbonate based PUs exhibit four types of C═O environments: hydrogen-bonded and non-hydrogen-bonded carbonyls in the urethane and carbonate portions of the chain structure. There are three observed absorbance peaks in this region: the absorbance at 1744 cm^{-1}

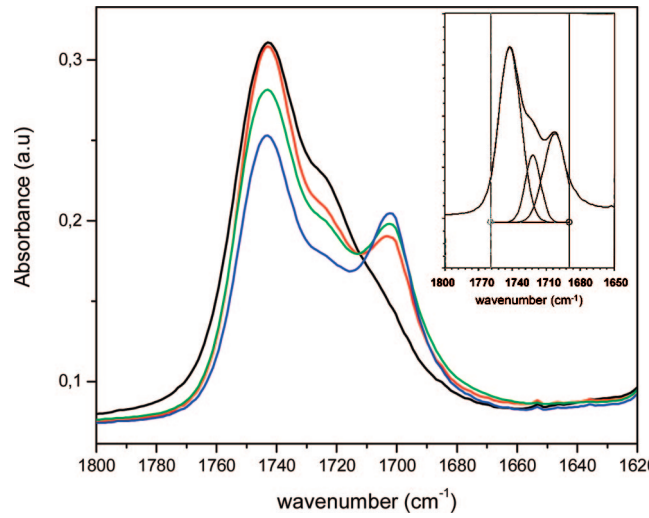

Figure 7. FT-IR spectra of the carbonyl region for PHEC−PUs: (black) PHEC-32.5, (red) PHEC-40, (green) PHEC-45, and (blue) PHEC-52. Inset: curve fitting for PHEC-40.

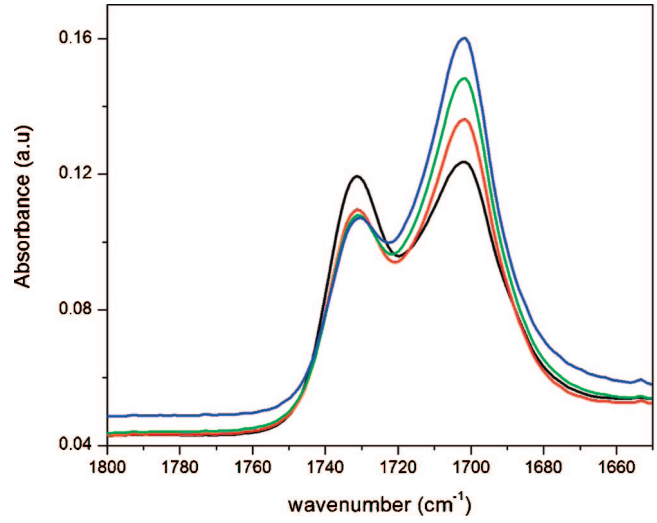

Figure 8. FT-IR spectra of the carbonyl region for PTMO−PUs: (black) PTMO-32.5, (red) PTMO-40, (green) PTMO-45, and (blue) PTMO-52.

can be assigned to the nonbonded carbonyls of the urethane and polycarbonate soft segments, the band at 1702 cm^{-1} to hydrogen-bonded urethane carbonyls, and the absorbance at 1723 cm^{-1} to the hydrogen-bonded carbonyls in the polycarbonate soft segments overlapped with loosely bonded urethane carbonyls.[30,38]

For most segmented polyurethanes, the hydrogen-bonded urethane carbonyl groups are associated with hard domains as "multimers"; thus, the carbonyl region exhibits only two bands, corresponding to "free" or non-hydrogen-bonded carbonyl groups and hydrogen-bonded "multimer" carbonyl groups.[39] That is the case for PTMO−PUs and (PDMS/PHMO)−PUs, whose carbonyl regions are represented in Figures 8 and 9, respectively. Non-hydrogen-bonded carbonyl groups exhibit maxima at 1731 cm^{-1} for PTMO-40 and 1735 cm^{-1} for (PDMS/PHMO)-40, whereas hydrogen-bonded carbonyl peaks are located at 1702 and 1704 cm^{-1} for PTMO-40 and (PDMS/PHMO)-40, respectively.

To compare the hydrogen-bonding characteristics of the three PU series under investigation here, only the fraction corresponding to hydrogen-bonded urethane carbonyls is considered, since the free urethane carbonyl groups cannot be compared

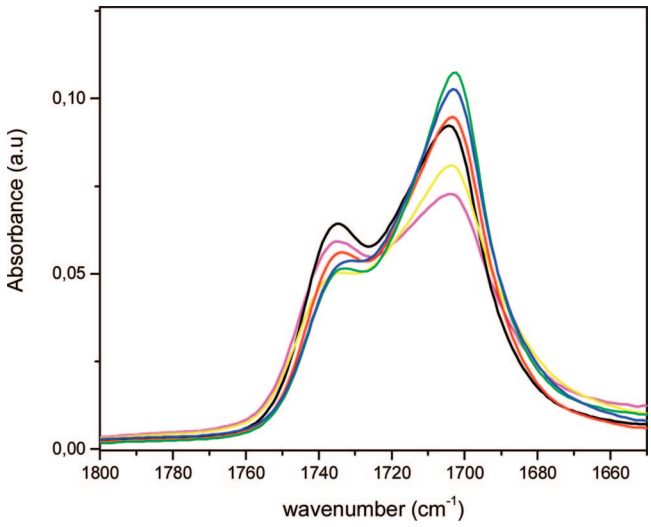

Figure 9. FT-IR spectra of the carbonyl region for (PDMS/PHMO)−PUs: (magenta) (PDMS/PHMO)-30, (black) (PDMS/PHMO)-32.5, (yellow) (PDMS/PHMO)-35, (red) (PDMS/PHMO)-40, (green) (PDMS/PHMO)-45, and (blue) (PDMS/PHMO)-52.

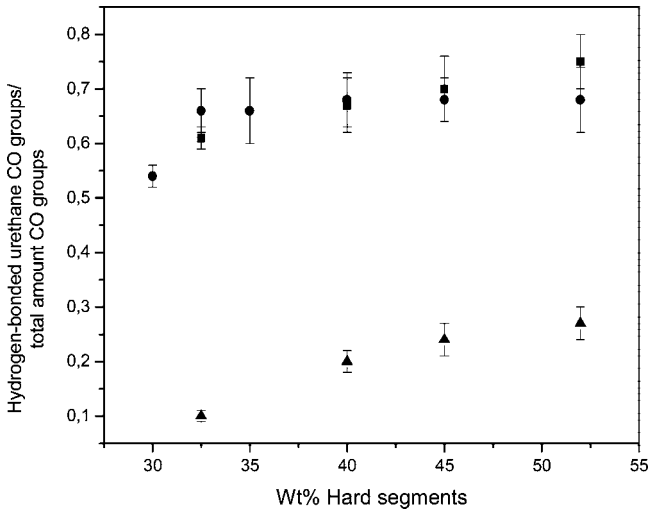

Figure 10. Fraction of hydrogen-bonded carbonyl groups as a function of the hard-segment content obtained from curve fitting: (●) (PDMS/PHMO)−PUs, (▲) PHEC−PUs, and (■) PTMO−PUs.

for the three series due to band overlap in the PHEC−PUs spectra. Figure 10 displays the relative amount of hydrogen-bonded urethane carbonyl groups obtained from curve fitting the carbonyl region as a function of the hard-segment concentration. The fraction of hydrogen-bonded PTMO−PU and (PDMS/PHMO)−PU urethane carbonyls are generally within experimental uncertainty and remain approximately constant with hard-segment concentration for both series. Degrees of phase separation for the three phase (PDMS/PHMO)−PUs are defined here on the basis of a pseudo-two-phase model, with the PDMS as one phase and all other components modeled as residing in a second hypothetical phase. In this way, we obtain information on the extent of PDMS phase separation (complete) but no direct information from SAXS on hard-domain organization. The FTIR results provide the important insight that hard domains in the (PDMS/PHMO) copolymers exhibit degrees of segregation/organization very much like hard domains in PTMO−PU copolymers. Finally, the relatively large fraction of H-bonded carbonyls for PTMO-52 is apparently inconsistent with lower bulk degrees of phase separation determined from SAXS. This very likely arises from differences in solidification history of the two samples and demonstrates the critical role that kinetics

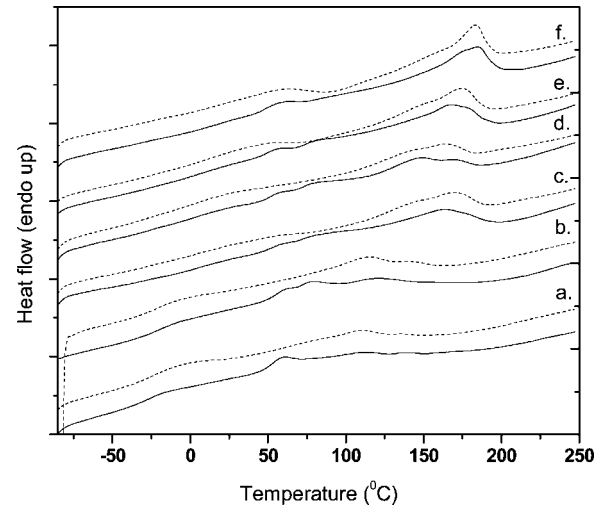

Figure 11. Representative DSC thermograms of the (PDMS/PHMO)−PUs: dotted lines correspond to the second run after rapidly cooling the sample to −90 °C at 100 °C/min: a, (PDMS/PHMO)-30; b, (PDMS/PHMO)-32.5; c, (PDMS/PHMO)-35; d, (PDMS/PHMO)-40; e, (PDMS/PHMO)-45; and f, (PDMS/PHMO)-52.

plays in determining unlike segment demixing in segmented polyurethane copolymers, particularly in the case of copolymers with high hard-segment contents.

PHEC−PUs exhibit a much lower fraction of hydrogen-bonded urethane carbonyl groups than the PTMO−PUs and (PDMS/PHMO)−PUs copolymers, in qualitative agreement with the results from SAXS. However, it is necessary to be cautious when considering these data. Since there are two bands overlapped at 1723 cm^{-1} (corresponding to hydrogen-bonded carbonate and non-hydrogen-bonded urethane carbonyls), the correction that takes into account the differences in absorptivity between non-hydrogen-bonded and hydrogen-bonded carbonyls is an approximation. Also, the total area corresponding to the carbonyl groups is higher than in the case of the PTMO and (PDMS/PHMO)−PUs due to the presence of carbonyl groups in the carbonate soft segments.

3.4. Phase Transitions. *(PDMS/PHMO)−PUs.* Representative thermograms corresponding to the first and second heating scans (the latter after rapid cooling from the homogeneous phase, from 250 to −120 °C) are represented in Figure 11 for the (PDMS/PHMO)−PUs. One expects a microphase-separated segmented block copolymer to exhibit two T_g's: one associated with an amorphous soft phase and the other with a hard phase. For microphase-separated PUs, mixing of short MDI−BDO blocks would raise the T_g of the soft phase. Although it is less likely that soft segments reside in hard domains, if this were to occur, it would lead to a reduction in hard-phase T_g.

The T_g of a relatively high molecular weight version of the neat hard segment, MDI−BDO, as reported in literature[24] and verified by us, is ∼110 °C. The neat α,ω-bis(6-hydroxyethoxypropyl) poly(dimethylsiloxane) diol exhibits two T_gs at −112 and −8 °C.[46] The first corresponds to the principle repeating unit ($Si(CH_3)_2O$), while the second corresponds to the hydroxyethoxypropyl end-group segments that, due to significant differences in chemical structure (i.e., solubility parameter) with the PDMS repeat unit, are segregated and form their own phase.

The PHMO macrodiol is a highly crystalline solid whose T_g is located at −35 °C. It is hypothesized that the T_gs observed for PU80−30 and PU80−32.5, clearly visible at −25 and −23 °C, respectively, correspond to a mixture of PHMO and PDMS end-group segments. To assess this possibility, we applied the Fox equation[40] $1/T_g = (w_{PHMO}/T_{gPHMO}) + (w_{PDMS\ end\ groups}/T_{gPDMS\ end\ groups})$, where w_{PHMO} and $w_{PDMS\ end\ groups}$ correspond to

Table 2. Temperatures and Enthalpies from the DSC Run after Rapid Cooling

	T_g (°C)	ΔC_p (J/g °C)	T_{MST}[a] (°C)	ΔH (J/g)	T_{MMT}[b] (°C)	ΔH (J/g)
			(PDMS/PHMO)−PUs			
(PDMS/PHMO)-30	−25	0.20			107	8.2
(PDMS/PHMO)-32.5	−23	0.23			113	9.6
(PDMS/PHMO)-35					159	11.5
(PDMS/PHMO)-40					159	10.2
(PDMS/PHMO)-45					173	15.4
(PDMS/PHMO)-52					183	16.2
			PHEC−PUs			
PHEC-32.5	0	0.44				
PHEC-40	8	0.38	54	−8.9	138	8.7
PHEC-45	15	0.34	66	−11.6	150	10.4
PHEC-52	25	0.35	68	−15.9	160	18.1
			PTMO−PUs			
PTMO-32.5	−37	0.16	30	−2.1	112	5.6
PTMO-40	−36	0.42	26	−2.9	147	12.4
PTMO-45	−37	0.26			165	15.4
PTMO-52	−27	0.15			175	18.0

[a] Microphase separation temperature [b] Microphase mixing temperature

the weight fractions of PHMO and the PDMS end-group segments, respectively. w_{PHMO} and $w_{PDMS\ end\ groups}$ were recalculated taking into account the initial composition of the soft segments [PDMS:PHMO 80:20 (w/w)]. The recalculated weight ratios for each of the components in the soft segments was PDMS:end-group segments:PHMO = 0.64:0.16:0.2. The mixture formed by 57 wt % PHMO (corresponding to the 0.2 portion) and 43 wt % of PDMS end-group segments (the 0.16 portion) is predicted to have a T_g of approximately −24 °C. This is near the experimental observations for PU80−30 and PU80−32.5 and suggests that there is little mixing between hard and polyether constituents for these copolymer compositions. It is not possible to determine the position of the soft phase T_g at HS concentrations higher than 32.5 wt %, although the soft phase α-transition is clearly observed in DMTA experiments and increases with the hard-segment concentration, indicating the mixing of some presumably relatively short, hard segments in the soft polyether phase.[21] Another factor that could influence T_g with respect to the neat macrodiols is that both the relatively low molecular weight PHMO and PDMS end-group segments are connected to hard segments, and one can envision that their motion is influenced by pinning by hard domains, raising the T_g.[41]

An endotherm at ∼50 °C is visible for all the samples in the first run. It is been proposed that this corresponds to single MDI linkages (lone MDI not chain extended with BDO),[42] although why such a transition should be observed [especially when such lone MDIs would be expected to reside in the (polyether) soft phase] is not at all clear. Temperature-dependent FTIR experiments should assist in assigning this transition, and we will present our conclusions in a future publication.

At temperatures higher than 100 °C, all (PDMS/PHMO) copolymers exhibit broad endotherms in both initial and second DSC thermograms, whose enthalpy and transition temperature increase with the HS concentration. The transition temperatures and associated enthalpies acquired during the second run are displayed in Table 2. One possibility is that this endotherm is associated, at least partly, with mixing between hard and soft segments, by analogy with MDI−BDO polyurethanes containing polyether soft segments.[43−46] In fact, loss of SAXS intensity, indicative of segment mixing, in our recent time-resolved SAXS studies of these copolymers was observed to occur at the end on the higher temperature DSC endotherm, supporting this assignment.[47] As a consequence, the peak temperature of the higher temperature endotherm is listed in Table as "T_{MMT}" (microphase mixing temperature).

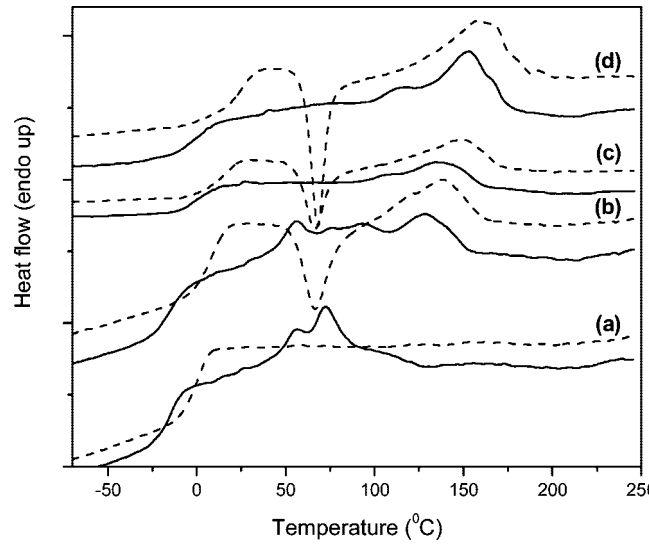

Figure 12. Representative DSC thermograms of the PHEC−PUs: dotted lines correspond to the second run after rapidly cooling the sample to −90 °C at 100 °C/min: a, PHEC-32.5; b, PHEC-40; c, PHEC-45; and d, PHEC-52.

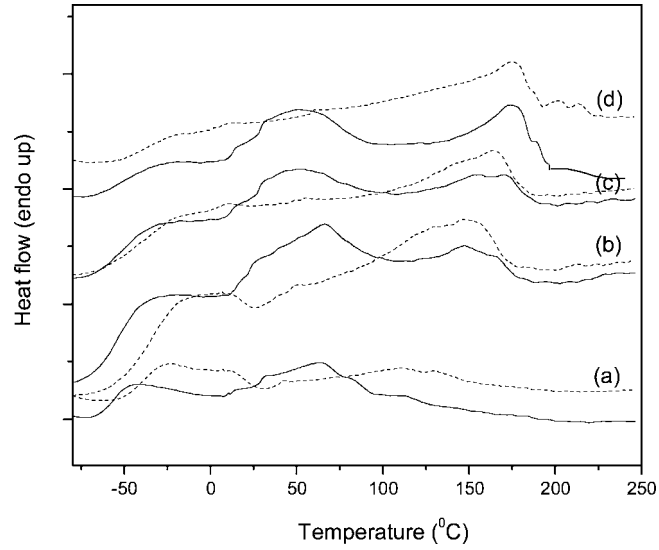

Figure 13. Representative thermograms of the PTMO−PUs: dotted lines correspond to the second run after rapidly cooling the sample to −90 °C at 100 °C/min: a, PTMO-32.5; b, PTMO-40; c, PTMO-45; and d, PTMO-52.

PHEC−PUs. Representative thermograms for the PHEC−PUs are displayed in Figure 12. A single T_g is observed in the initial run, whose temperature increases with the hard-segment concentration and can be reasonably assigned to the soft phase. Similar to the (PDMS/PHMO)−PUs, the T_g corresponding to the soft phase is higher than that of the neat macrodiol for all hard-segment concentrations (T_g of the PHEC diol = −70 °C).

At hard-segment concentrations ≤40%, the first run displays a broad endotherm around 70 °C, which could also be a T_g overlapped with an endotherm assigned to short, hard-segment sequences. It is worth mentioning that the probability of formation of short sequences decreases with the hard-segment concentration, which would explain the absence of this endotherm for hard-segment concentrations ≥40%.

At temperatures higher than 100 °C, copolymers with hard-segment concentrations ≥40% exhibit a broad endotherm whose enthalpy and transition temperature increases with hard-segment

concentration. As for the (PDMS/PHMO)−PU copolymers, time-resolved SAXS measurements provide evidence that this transition can be at least partly assigned to mixing of hard and soft segments.[47]

After rapidly cooling these copolymers from 250 to −90 °C, both the T_g and the ΔC_p associated with the soft-phase transition increase with respect to that determined in the first run. This suggests mixing of at least some, presumably relatively short, hard-segment sequences in the soft phase (see Table 2), i.e., incomplete hard/soft-segment segregation on rapid cooling. This is reinforced by the absence of the endotherm assigned to short, hard sequences in PHEC-32.5 and PHEC-40 in the second run.

As seen in Figure 12, at hard-segment concentrations ≥40%, the thermograms of PHEC copolymers exhibit an exotherm immediately preceding an endotherm having approximately the same transition enthalpy. This observation strongly supports the idea that the exotherm and endotherm represent hard- and soft-phase demixing and mixing, respectively. The peak temperature of the exotherm is listed in Table 2 as "T_{MST}" (microphase separation temperature). Similar behavior has been observed for other polyurethanes.[43,48,49] For poly(ester urethanes) in which the soft segments can form hydrogen bonds with urethane hard segments, such behavior has been rationalized by invoking intersegment interactions as impeding the demixing process on rapid cooling.[49]

PTMO−PUs. The DSC thermograms for the PTMO−PUs are presented in Figure 13. The trends observed for the soft-segment T_g after rapid cooling are similar to those of the PHEC−PUs copolymers. That is, T_gs for all copolymers are higher with respect to the neat PTMO macrodiol ($T_g = -45$ °C) and ΔC_p increases relative to the first run. However, the T_gs remain approximately constant for all the hard-segment concentrations except for PTMO-52.

At temperatures between 50 and 100 °C, the initial thermograms of all PTMO−PUs exhibit a broad endotherm that appears to be overlapped with a ΔC_p change (i.e., a T_g) at around 50 °C. However, this feature is absent after rapid cooling and is in keeping with the assignment of this endotherm to short, hard-segment sequences. For the rapidly cooled PTMO copolymers, endotherms appear at temperatures higher than 100 °C that can be assigned to intersegment mixing, by analogy to other studies on poly(ether urethanes). Rapidly cooled PTMO-32.5 and PTMO-40 exhibit relatively shallow exothermic behavior immediately followed by an endotherm, but its enthalpy is much higher than that associated with the exotherm (see Table 2). This confirms that hard/soft-segment demixing during rapid cooling to low temperatures is more rapid for PTMO−PUs compared to PHEC−PUs.

Summary

The degree of hard/soft-segment demixing is quantified and compared for three series of well-defined segmented polyurethanes, and our results demonstrate that the chemistry of the soft segment plays a critical role in the phase organization of PUs copolymers having the same hard-segment chemistry. (PDMS/PHMO)-based copolymers exhibit a three-phase, core−shell morphology, while the other copolymers exhibit a typical two-phase structure consisting of a soft phase (composed of PTMO or PHEC, lone MDI units, and some dissolved, relatively short, hard segments) and a hard phase composed of hard segments. AFM phase images demonstrate that the hard domains in each copolymer series exhibit a noncontinuous morphology of dimension of approximately 50−75 nm^2. SAXS experiments demonstrate that PTMO−PUs exhibit a higher degree of phase separation than PHEC-based copolymers, except at high hard-segment concentrations at which demixing kinetics strongly influence phase separation. This was explained by differences in intersegment hydrogen bonding between the hard and soft segments.

Quantification of hydrogen-bonded urethane carbonyls by FTIR spectroscopy also assists comparison of the three PU copolymer series. Analysis of the FTIR spectra of the (PDMS/PHMO) copolymers suggests degrees of hard-segment phase separation very much like that in PTMO−PU copolymers. PHEC-based copolymers exhibit a much lower fraction of hydrogen-bonded urethane carbonyl groups, in qualitative agreement with SAXS results.

The interactions between hard and soft segments in PHEC−PUs results in slower demixing on rapid cooling, compared to PTMO and (PDMS/PHMO) copolymers. Except for PHEC-32.5, all copolymers exhibit a broad endotherm at temperatures above 100 °C, whose temperature and enthalpy increase with the hard-segment content. Time-resolved SAXS experiments that will be reported in a future publication[47] demonstrate that this transition is at least partly associated with mixing between hard and soft segments for all three copolymer series.

Acknowledgment. The authors would like to express their appreciation to Prof. Paul Painter for helpful discussions regarding interpretation of FTIR spectra.

Supporting Information Available: This material is available free of charge via the Internet at http://pubs.acs.org.

References and Notes

(1) Gibson, P. E.; Vallence, M. A.; Cooper, S. L. In *Development in Block Copolymers-1*; Elsevier: London, 1982; p 217.
(2) Velankar, S.; Cooper, S. L. *Macromolecules* **1998**, *31*, 9181.
(3) Velankar, S.; Cooper, S. L. *Macromolecules* **2000**, *33*, 382.
(4) Clough, S. B.; Schneider, N. S.; King, A. O. *J. Macromol. Sci., Phys.* **1968**, *B2*, 553.
(5) Van Bogart, J. W. C.; Lilaonitkul, A.; Cooper, S. L. *ACS Adv. Chem. Ser.* **1979**, *176*, 3.
(6) Gunatillake, P. A.; Meijs, G. F.; McCarthy, S. J.; Adhikari, R.; Sherriff, N. *J. Appl. Polym. Sci.* **1998**, *69*, 1621.
(7) Tang, Y. W.; Labow, R. S.; Santerre, J. P. *J. Biomed. Mater. Res.* **2001**, *57*, 597.
(8) Revenko, I.; Tang, Y.; Santerre, J. P. *Surf. Sci.* **2001**, *491*, 346.
(9) Christenson, E. M.; Dadsetan, M.; Wiggins, M.; Anderson, J. M.; Hiltner, A. *J. Biomed. Mat. Res.* **2004**, *69*, 407.
(10) Garrett, J. T.; Siedlecki, C. A.; Runt, J. *Macromolecules* **2001**, *34*, 7066.
(11) McLean, R. S.; Sauer, B. B. *Macromolecules* **1997**, *30*, 8314.
(12) Sheth, J. P.; Aneja, A.; Wilkes, G. L.; Yilgor, E.; Atilla, G. E.; Yilgor, I.; Beyer, F. L. *Polymer* **2004**, *45*, 6919.
(13) Sheth, J. P.; Yilgor, E.; Erenturk, B.; Ozhalici, H.; Yilgor, I.; Wilkes, G. L. *Polymer* **2005**, *46*, 8185.
(14) Yilgor, I.; Shaaban, A. K.; Steckle, W. P.; Tyagi, D.; Wilkes, G. L.; McGrath, J. E. *Polymer* **1984**, *25*, 1800.
(15) Tyagi, D.; Yilgor, I.; McGrath, J. E.; Wilkes, G. L. *Polymer* **1984**, *25*, 1807.
(16) Tyagi, D.; Wilkes, G. L.; Yilgor, I.; McGrath, J. E. *Polym. Bull.* **1982**, *8*, 543.
(17) Tyagi, D.; McGrath, J. E.; Wilkes, G. L. *Polym. Eng. Sci.* **1986**, *26*, 1371.
(18) Chen, T. K.; Chui, J. Y.; Shieh, T. S. *Macromolecules* **1997**, *30*, 5068.
(19) Li, C.; Yu, X.; Speckhard, T. A.; Cooper, S. L. *J. Polym. Sci.: Polym. Phys.* **1988**, *26*, 315.
(20) Gunatillake, P. A.; Meijs, G. F.; McCarthy, S. J.; Adhikari, R. *J. Appl. Polym. Sci.* **2000**, *76*, 2026.
(21) Hernandez, R.; Weksler, J.; Padsalgikar, A.; Runt, J. *Macromolecules* **2007**, *40*, 5441.
(22) Bonart, R.; Mueller, E. H. *J. Macromol. Sci., Phys.* **1974**, *B 10*, 345.
(23) Bonart, R.; Mueller, E. H. *J. Macromol. Sci., Phys.* **1974**, *B 10*, 177.
(24) Leung, L. M.; Koberstein, J. T. *J. Polym. Sci. Polym. Phys. Edn.* **1985**, *23*, 1883.
(25) Garrett, J. T.; Lin, J. S.; Runt, J. *Macromolecules* **2002**, *35*, 161.
(26) Garrett, J. T.; Runt, J.; Lin, J. S. *Macromolecules* **2000**, *33*, 6353.
(27) Saiani, A.; Rochas, C.; Eeckhaut, G.; Daunch, W. A.; Leenslag, J. W.; Higgins, J. S. *Macromolecules* **2004**, *37*, 1411.
(28) Hernandez, R.; Weksler, J.; Padsalgikar, A.; Runt, J. *J. Biomed. Mat. Res.* **2008**, *87A*, 546.
(29) Peebles, L. H. *Macromolecules* **1976**, *9*, 58.

(30) Coleman, M. M.; Lee, K. H.; Skrovanek, D. J.; Painter, P. C. *Macromolecules* **1986**, *19*, 2149.
(31) Skrovanek, D. J.; Painter, P. C.; Coleman, M. M. *Macromolecules* **1986**, *19*, 699.
(32) Koberstein, J. T.; Stein, R. S. *J. Polym. Sci.: Polym. Phys.* **1983**, *21*, 1439.
(33) Velankar, S.; Cooper, S. L. *Macromolecules* **2000**, *33*, 382.
(34) Fredrickson, G. H.; Milner, S. T.; Leibler, L. *Macromolecules* **1992**, *25*, 6341.
(35) Coleman, M. M.; Graf, J. F.; Painter, P. C. *Specific Interactions and the Miscibility of Polymer Blends*; Technomic: Lancaster, 1991.
(36) Sung, C. S. P.; Schneider, N. S. *Macromolecules* **1975**, *8*, 68.
(37) Garrett, J. T.; Xu, R.; Cho, J.; Runt, J. *Polymer* **2003**, *44*, 2711.
(38) Christenson, E. M.; Anderson, J. M.; Hiltner, A. *J. Biomed. Mater. Res.* **2004**, *70A*, 245.
(39) Mattia, J.; Painter, P. C. *Macromolecules* **2007**, *40*, 1546.
(40) Fox, T. G. *Bull. Am. Phys. Soc.* **1965**, *1*, 123.
(41) Kyritsis, A.; Pissis, P.; Mai, S. M.; Booth, C. *Macromolecules* **2000**, *33*, 4581.
(42) Martin, D. J.; Meijs, G. F.; Renwick, G. M.; McCarthy, S. J.; Gunatillake, P. A. *J. Appl. Polym. Sci.* **1996**, *62*, 1377.
(43) Saiani, A.; Daunch, W. A.; Verbeke, H.; Leenslag, J. W.; Higgins, J. S. *Macromolecules* **2001**, *34*, 9059.
(44) Seymour, R. W.; Cooper, S. L. *Macromolecules* **1973**, *6*, 48.
(45) Koberstein, J. T.; Russell, T. R. *Macromolecules* **1986**, *19*, 714.
(46) Koberstein, J. T.; Galambos, A. F. *Macromolecules* **1992**, *25*, 5618.
(47) Pongkitwitoon, S.; Hernandez, R.; Weksler, J.; Padsalgikar, A; Runt, J. To be submitted for publication.
(48) Chen, T. K.; Shieh, T. S.; Chui, J. Y. *Macromolecules* **1998**, *31*, 1312.
(49) Wilkes, G. L.; Wildnauer, R. *J. Appl. Phys.* **1975**, *46*, 4148.

MA8014454